Proceedings of the 2002 IEEE
International Conference on Robotics & Automation
Washington, DC • May 2002

Design of a Four-Wheeled Omnidirectional Mobile Robot with Variable Wheel Arrangement Mechanism

Kyung-Seok Byun, Sung-Jae Kim, Jae-Bok Song

Department of Mechanical Engineering, Korea University
5-ga, Anam-dong Sungbuk-gu, Seoul, 136-701, Korea.
E-mail: jbsong@korea.ac.kr

Abstract

An omnidirectional mobile robot equipped with four independent omnidirectional wheels can perform 3 DOF motion and has one redundant DOF. This redundancy can be used to drive the mechanism enabling the wheel arrangement to vary, which can function as a continuously -variable transmission (CVT). In this research, a special mechanism called a variable wheel arrangement mechanism is proposed to increase the range of velocity ratio for the CVT from the wheel velocities to robot velocity, which may improve performance of the mobile robot. The mobile robot with this mechanism was constructed and various tests have been conducted to demonstrate the validity and feasibility of the proposed mechanism.

1. Introduction

Omnidirectional mobile robots are capable of moving in an arbitrary direction without changing the direction of wheels, because they can achieve 3 DOF motion on a two-dimensional plane. Various types of omnidirectional mobile robots have been proposed so far; universal wheels [1, 2], ball wheels [3], off-centered wheels [4] are popular among them.

The omnidirectional mobile robots using omnidirectional wheels composed of passive rollers or balls usually have 3 or 4 wheels. The three-wheeled omnidirectional mobile robots are capable of achieving 3 DOF motions by driving 3 independent actuators [5, 6], but they may have stability problem due to the triangular contact area with the ground, especially when traveling on a ramp with the high center of gravity owing to the payload they carry. It is desirable, therefore, that four-wheeled vehicles be used when stability is of great concern [7]. However, independent drive of four wheels creates one extra DOF. To cope with such a redundancy problem, the mechanism capable of driving four omnidirectional wheels using three actuators was suggested [8].

Another approach to a redundant DOF is to devise some mechanism which uses this redundancy to change wheel arrangements [9, 10]. Since the relationship between the robot velocity and wheel velocities depends on wheel arrangement, varying wheel arrangement can function as a transmission. Furthermore, it can be considered as a continuously-variable transmission (CVT), because the robot velocity can change continuously by adjustment of wheel arrangements without employing a gear train. The CVT can provide more efficient motor driving capability as its range of velocity ratio get wider. The mobile robot proposed by Wada [9], however, has a limited range to ensure stability of the vehicle.

In this paper, a new mechanism so-called variable wheel arrangement mechanism (VWAM) is proposed in which robot stability is guaranteed regardless of wheel arrangement and thus the range of velocity ratio is greatly extended. The four-wheeled omnidirectional mobile robot involving this mechanism combined with the continuous alternate wheels developed in our laboratory [11] has been developed. In the remaining sections, the kinematic and dynamic analysis of the proposed mobile robot is performed and various test results are presented demonstrate the validity and feasibility of the proposed mechanism.

2. Variable Wheel Arrangement Mechanism

In this section, the structure and operational principle of the proposed variable wheel arrangement mechanism (VWAM) will be presented. In addition, comparison of this mechanism with the variable footprint mechanism (VFM) proposed by Wada is discussed below.

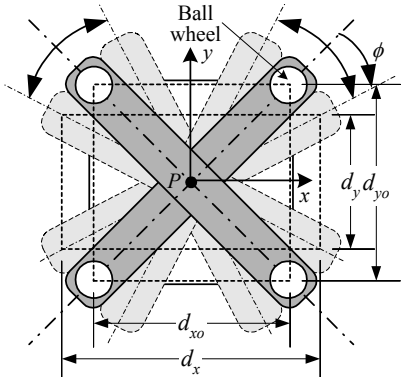

Fig. 1 Variable footprint mechanism for CVT [9].

Figure 1 shows the variable footprint mechanism in which two beams can rotate at a pivot joint P in the middle [9]. Note that the two beams are constrained to rotate in a symmetric fashion with a single DOF by means of differential gears at the pivot. The ball wheels and motors are mounted at each end of the beams. Meanwhile,

the variable wheel arrangement mechanism (VWAM) developed in this research is illustrated in Fig. 2. The wheel module consists of the omnidirectional wheel called a continuous alternate wheel developed in our laboratory [11] (see Fig. 6), an individual motor and steering link. Notice that the four wheel modules can rotate about each pivot point C_1, .., C_4 located at the corners of the robot body, but they are constrained to have a synchronized steering motion of 1 DOF by the VWAM comprising the connecting links and linear guide.

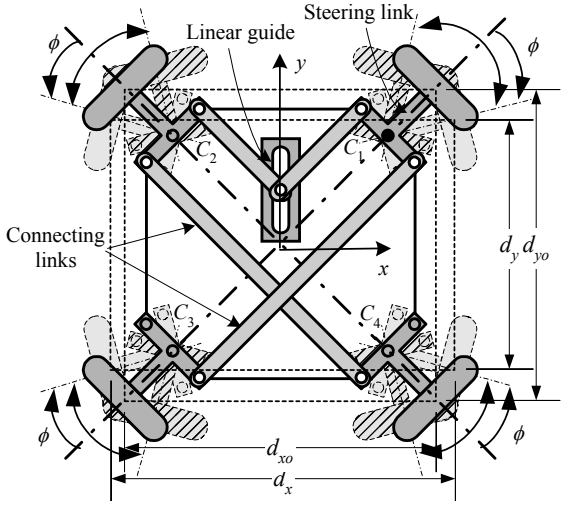

Fig. 2 Variable wheel arrangement mechanism for CVT.

In Figures 1 and 2, the steering angle ϕ is defined as the angle from the zero position in which the beams (Fig. 1) or the lines (i.e., C_1C_3 or C_2C_4) connecting the centers of diagonally opposed wheels (Fig. 2) coincide with the diagonal lines of the robot body. The wheelbases, the distances between the centers of two adjacent wheels on the x- and y-axis, at the configuration $\phi = 0$ are denoted as d_{xo} and d_{yo}. If the robot body is square, then $d_{xo} = d_{yo}$.

In Fig. 1 the rotation center of the wheel module is located at the intersection P of the two beams. As the steering angle ϕ becomes large, therefore, one side of the rectangle whose vertices are wheel-ground contact points may get excessively smaller than the other side, thus leading to increased instability. Hence the steering angle was limited to the range between -17.5° and $+17.5^{\circ}$, which causes the range of velocity ratio (defined in Section 4) to be limited. On the contrary, since the wheel modules in Fig. 2 rotate about each pivot joint C_1, .., C_4 placed at the corners of a robot platform, the robot is structurally stable even for a large steering angle. As a result of this feature, the steering angle can be substantially large, and thus the range of velocity ratio increases accordingly. Figure 3 shows various wheel arrangements using the variable wheel arrangement mechanism.

Let us define the wheelbase ratio as follows:

$$r_{wb} = \frac{\min(d_x, d_y)}{d_{xo}} \tag{1}$$

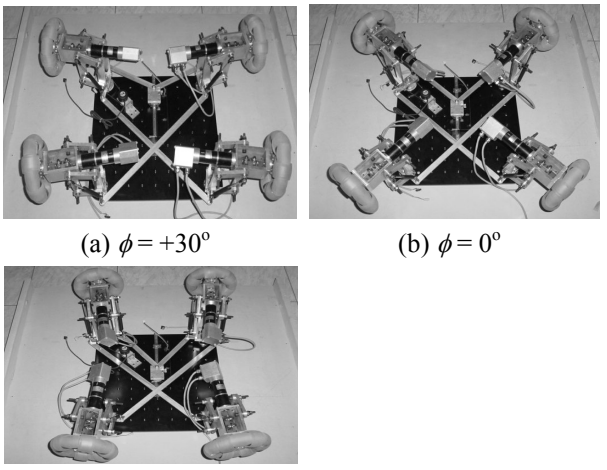

(a) $\phi = +30^{\circ}$ (b) $\phi = 0^{\circ}$

(c) $\phi = -30^{\circ}$

Fig. 3 Various wheel arrangements using variable wheel arrangement mechanism.

where d_x and d_y represent the wheelbase (i.e., the distance between the wheel centers) in the x and y directions as shown in Fig. 2. Figure 4 illustrates the wheelbase ratios for the two mechanisms as a function of the steering angle. As shown in the figure, the proposed variable wheel arrangement provides a much wider range of steering angle without degrading stability, since the change in r_{wb} is smaller than that for the variable footprint mechanism.

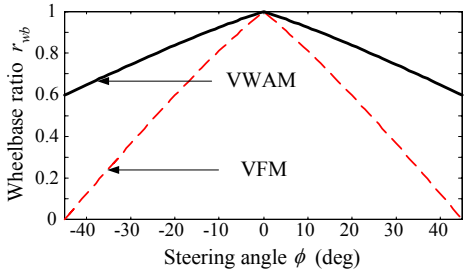

Fig. 4 Comparison of wheelbase ratios for variable wheel arrangement mechanism (VWAM) and variable footprint mechanism (VFM).

3. Kinematic and Dynamic Analysis of a Robot

3.1 Kinematic analysis

The four-wheeled omnidirectional mobile robot is illustrated in Fig. 5. This schematic is a simplified version of VWAM in Fig. 2 for convenience, which yields the same geometric analysis as the mechanism in Fig. 2. The frame O-XY is assigned as a reference frame for the robot motion in the plane and the moving frame o-xy is attached to the robot center. On the other hand, the angle θ between the y-axis and the diagonal line of the robot

platform depends on the shape of a platform. (i.e., $\theta = 45^o$ for the square platform)

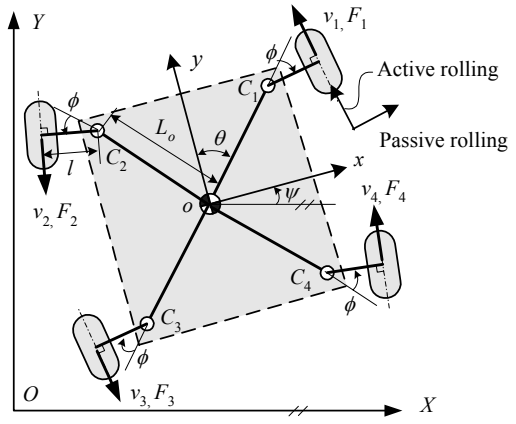

Fig. 5 Coordinate systems for omnidirectional mobile robot under consideration

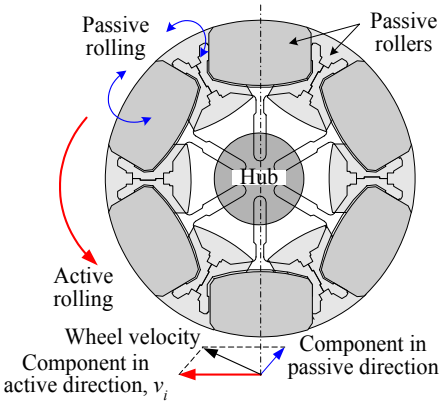

Fig. 6 Appearance of continuous alternate wheel and active and passive rolling.

Since the omnidirectional wheel under consideration shown in Fig. 6 consists of a circular hub surrounded by passive rollers, it has two modes of motion: active rolling and passive rolling [12]. In active rolling the wheel rotates about the hub axis by the wheel actuator with the rollers remain still, while in passive rolling the wheel translates in the direction of the hub axis with the roller in contact with the ground spinning and the hub fixed. Motion in other directions involves a combination of hub rotation and roller rotation. Thus the wheel velocity can be decomposed into the component in the active direction (i.e., v_i) and the one in the passive direction.

The relationship between the wheel velocity vector and vehicle velocity vector can be expressed from the geometry in Fig. 5 by

$$\begin{Bmatrix} v_1 \\ v_2 \\ v_3 \\ v_4 \end{Bmatrix} = \begin{bmatrix} -C & S & L & -l \\ -C & -S & L & l \\ C & -S & L & -l \\ C & S & L & l \end{bmatrix} \begin{Bmatrix} v_x \\ v_y \\ \dot{\psi} \\ \dot{\phi} \end{Bmatrix} \tag{2}$$

where $C = \cos(\phi + \theta)$, $S = \sin(\phi + \theta)$, $L = L_o \cos\phi + l$. Here, v_1, v_2, v_3, v_4 are the wheel velocities in the active direction, v_x and v_y are the translational velocities of the robot center, $\dot{\psi}$ is the angular velocity about the robot center, and $\dot{\phi}$ is the derivative of the steering angle, respectively. The matrix in Eq. (2) is invertible, provided $0 < \phi + \theta < 90^o$ since $C \neq 0$ and $S \neq 0$. Then the following inverse matrix is obtained, which corresponds to the Jacobian matrix relating the wheel velocity vector to the robot velocity vector:

$$\mathbf{J} = \frac{1}{4} \begin{bmatrix} -1/C & -1/C & 1/C & 1/C \\ 1/S & -1/S & -1/S & 1/S \\ 1/L & 1/L & 1/L & 1/L \\ -1/l & 1/l & -1/l & 1/l \end{bmatrix} \tag{3}$$

Using this Jacobain matrix, the relationship between the wheel velocities and robot velocity are given by

$$\mathbf{V}_w = \mathbf{J}^{-1}\mathbf{V}_r, \quad \mathbf{V}_r = \mathbf{J}\,\mathbf{V}_w \tag{4}$$

where $\mathbf{V}_w = [v_1 \;\; v_2 \;\; v_3 \;\; v_4]^T$, $\mathbf{V}_r = [v_x \;\; v_y \;\; \dot{\psi} \;\; \dot{\phi}]^T$

It follows from Eq. (4) that the robot velocity and the steering velocity of the variable wheel arrangement mechanism can be completely determined by control of four independent motors driving each wheel.

3.2 Dynamic analysis

The equation of dynamics for the robot under consideration can be written by

$$M(\dot{v}_x - v_y\dot{\psi}) = F_x \tag{5a}$$

$$M(\dot{v}_y + v_x\dot{\psi}) = F_y \tag{5b}$$

$$I_z\ddot{\psi} = T_z \tag{5c}$$

where M is the mass of the robot, I_z the moment of inertia about the z axis passing through the center of gravity (c.g.), F_x and F_y are the forces acting on the c.g., and T_z is the moment acting on the c.g. about the z axis, respectively. The force and moment can be expressed from the geometry in Fig. 5 by

$$\begin{aligned} F_x &= -CF_1 - CF_2 + CF_3 + CF_4 \\ F_y &= SF_1 - SF_2 - SF_3 + SF_4 \\ T_z &= LF_1 + LF_2 + LF_3 + LF_4 \\ T_\phi &= -lF_1 + lF_2 - lF_3 + lF_4 \end{aligned} \tag{6}$$

where T_ϕ is the torque required to rotate the wheel module. Note that the force F_i (i = 1, .., 4) is the traction force acting on the wheel in the direction of active rolling. Using the Jacobian matrix defined in Eq. (3), the relationship between the wheel traction forces and the

resultant force acting on the robot is given by

$$\mathbf{F}_r = \mathbf{J}^{-T}\mathbf{F}_w, \quad \mathbf{F}_w = \mathbf{J}^T\mathbf{F}_r \tag{7}$$

where $\mathbf{F}_w = [F_1 \;\; F_2 \;\; F_3 \;\; F_4]^T, \mathbf{F}_r = [F_x \;\; F_y \;\; T_z \;\; T_\phi]^T$.

It is noted that $\mathbf{F}_r$ is given by the vectorial sum of the traction forces. Varying the combination of the traction forces can generate an arbitrary force and moment driving the vehicle and the moment steering the wheel modules.

4. CVT Using VWAM

4.1 Velocity and force ratios

Since the omnidirectional mobile robot is of 3 DOFs in the 2-D plane, it is difficult to define the velocity ratio in terms of scalar velocities. Thus the velocity ratio is defined using the concept of norms as follows:

$$r_v = \frac{\|\mathbf{V}_r\|}{\|\mathbf{V}_w\|} = \frac{\|\mathbf{J}\mathbf{V}_w\|}{\|\mathbf{V}_w\|} \tag{8}$$

Note that the velocity ratio for the identical wheel velocities varies depending on the steering angle. The maximum and minimum values of the velocity ratio can be computed from the singular value decomposition (SVD).

$$\mathbf{J} = \mathbf{U}\Sigma\mathbf{V}^T = \begin{bmatrix} 1 & 0 & 0 & 0 \\ 0 & 1 & 0 & 0 \\ 0 & 0 & 1 & 0 \\ 0 & 0 & 0 & 1 \end{bmatrix} \cdot \begin{bmatrix} 1/2C & 0 & 0 & 0 \\ 0 & 1/2S & 0 & 0 \\ 0 & 0 & 1/2L & 0 \\ 0 & 0 & 0 & 1/2l \end{bmatrix} \cdot \begin{bmatrix} -1/2 & -1/2 & 1/2 & 1/2 \\ 1/2 & -1/2 & -1/2 & 1/2 \\ 1/2 & 1/2 & 1/2 & 1/2 \\ 1/2 & -1/2 & 1/2 & -1/2 \end{bmatrix} \tag{9}$$

where the diagonal elements of $\mathbf{\Sigma}$ are the singular values of $\mathbf{J}$, and $\mathbf{U}$ and $\mathbf{V}$ are unitary matrices. Note that $1/2C$ and $1/2S$ are the translational velocity ratios in the x and y axes, and $1/2L$ is the rotational velocity ratio, respectively. Therefore, the velocity ratio can be represented by the ellipsoid whose axes are $1/2C$, $1/2S$, and$1/2L$ in the x, y, and z directions.

Figure 7 shows the velocity ratio profiles as a function of steering angle in the case of L_o = 0.283m, l = 0.19m, and θ = 45°. It is observed that the translational velocity ratios vary significantly in the range between 0.5 and infinity, while the rotational velocity ratio is kept nearly constant. When the steering angle is within the range between $-\phi_{\max}$ and $+\phi_{\max}$ ($0° < \phi_{\max} < 45°$), the ratios of maximum to minimum velocity ratios are given by

$$\alpha_x = \frac{\cos(45° - \phi_{\max})}{\cos(45° + \phi_{\max})}, \quad \alpha_y = \frac{\sin(45° + \phi_{\max})}{\sin(45° - \phi_{\max})}$$

$$\alpha_z = \frac{L_o \cos\phi_{\max} + l}{L_o + l} \tag{10}$$

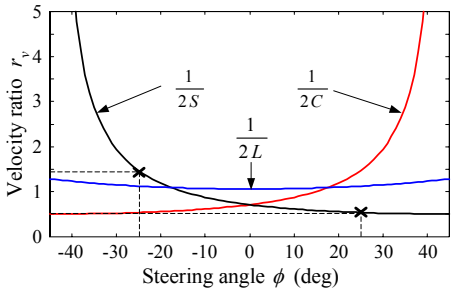

Fig. 7 Velocity ratio as a function of steering angle.

For example, if the steering angle varies from –25° to +25°, the velocity ratio in the y direction varies from 1.46 and 0.532, thus yielding α_y = 2.75. It is observed that the range of velocity ratio becomes wide as the steering angle grows in either sense.

The force ratio of the force acting on the robot center to the wheel traction force can be defined in the same way as the velocity ratio in Eq. (8) as follows:

$$r_f = \frac{\|\mathbf{F}_r\|}{\|\mathbf{F}_w\|} = \frac{\|\mathbf{J}^{-T}\mathbf{F}_w\|}{\|\mathbf{F}_w\|} = \frac{1}{r_v} \tag{11}$$

Note that the force ratio corresponds to the inverse of the velocity ratio. Figure 8 shows the force ratio as a function of steering angle. It is observed that the force ratio becomes maximum in one direction while minimum in the other direction as the steering angle reaches its maximum magnitude $\phi_{\max}$. Therefore, the steering angle should be determined so that the robot force to meet given specifications is generated.

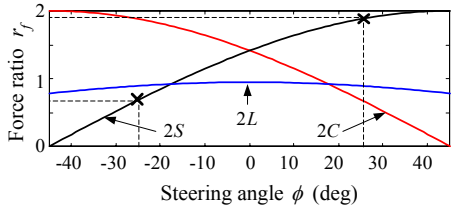

Fig. 8 Force ratio as a function of steering angle.

4.2 Selection of motors

A motor has an operating region in which continuous operation is guaranteed as shown in Fig. 9. This region is delimited by various factors such as maximum permissible speed, maximum continuous torque, and power rating. Most motors have characteristics of low torques and high speeds, which corresponds to region I (*a-d-e-l*). Use of a speed reducer combined with the motor can modify the operating region to region II (*a-b-m-n-k-a*) by lowering speeds and amplifying torques. When the

transmission device such as the CVT mechanism is added to the system, the operating region can be further extended to regions III (*a-c-f-i-j-a*).

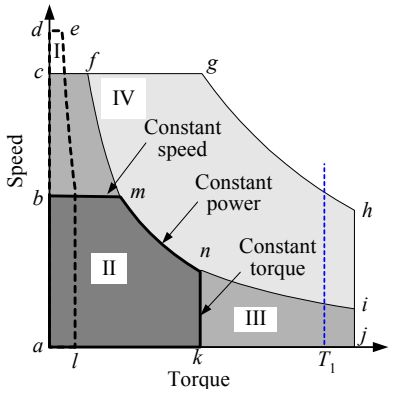

Fig. 9 Operating regions of motor (I: motor, II: motor + speed reducer, III: motor + speed reducer + CVT, IV: large motor + speed reducer)

Typical performance indices such as the maximum velocity, maximum acceleration, and gradability can be improved with the extended operating regions in that smaller motors can be used to meet the given performance specifications. For example, let T_1 be the torque required to meet the specification. It is clear that this torque cannot be obtained by use of the speed reducer alone since the operating region is limited to region II. One way to obtain this torque is to use the larger motor combined with a speed reducer, which extends the operating region to region IV (*a-c-g-h-j-a*). Addition of the CVT, however, enables the torque T_1 to be available even with the smaller motor combined with the speed reducer belonging to region II. It is noted that the size of a motor can be made smaller with the increased range of transmission ratio of the CVT, which justifies the proposed mechanism which can substantially increase the range of transmission ratio.

Referring to Fig. 7 and 8, when the steering range is $-17.5^{o} \sim +17.5^{o}$ in the variable footprint mechanism [9], the ranges of the translational velocity ratio and force ratios are 0.56 ~ 1.08 and 1.79 ~ 0.925, respectively, thereby resulting in the ratio of 1.93 (i.e., 1.79/0.925 or 1.79/0.925). On the other hand, when the steering range extends to $-30^{o} \sim +30^{o}$ in the proposed mechanism, the ranges of the translational velocity ratio and force ratios are extended to 0.52 ~ 1.93 and 1.93 ~ 0.52, respectively, thereby resulting in the ratio of 3.71 (i.e., 1.93/0.52). An increase in the steering range by an angle of 12.5^{o} can yield an increase in the robot performance by a factor of 1.93, which justifies the advantage of the proposed mechanism.

5. Construction of Mobile Robot

The omnidirectional mobile robot with the proposed variable wheel arrangement mechanism was designed and constructed as shown in Fig. 10. This robot contains the wheel module comprising the four omnidirectional wheels connected to the individual motors, variable wheel arrangement mechanism, a square platform whose side is 500mm. The height of the platform from the ground is 330mm, and the motor drives and controller are placed in this space between the platform and ground.

The omnidirectional wheels used in the constructed mobile robot are called the continuous alternate wheel, where inner and outer rollers are arranged continuously, thus resulting in no gap between the rollers [11]. These wheels are connected to the DC motors through universal joints. A wheel suspension system is required to ensure that the wheels are in contact with the ground at all times. This suspension can also absorb the shock transmitted to the wheels.

Figure 11 illustrates the control systems for the mobile robot. DSP (TMS320C32) is used as a master controller, while the micro-controller 80196KC is employed as a motor driver. The mobile robot can move autonomously, but the PC is used to monitor the whole system and collect data. The master controller plans the robot trajectory and commands the appropriate signal depending on the type of operation (i.e., speed mode or torque mode) to the motor drives where motor control is performed.

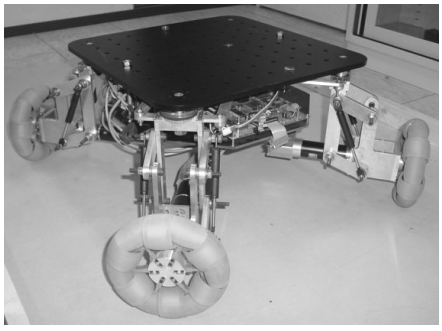

Fig. 10 Omnidirectional mobile robot

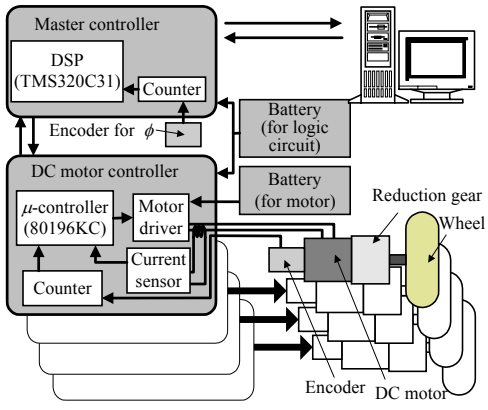

Fig. 11 Control systems for mobile robot

6. Experiments and Discussions

Various tests have been conducted to demonstrate performance of the constructed omnidirectional mobile robot equipped with the variable wheel arrangement mechanism. First, the steering angle was commanded to vary from -30^{o} to 30^{o} gradually with the wheel velocities held constant and then the translational velocities v_x and v_y and angular velocity $\dot{\psi}$ were measured. The computed velocity ratios from the measurements are plotted against the steering ratio in Fig. 12. Close agreement between the theoretical values (represented by solid lines) and measured values (marked by 'x') is observed. It is also noticed that the range of velocity ratio becomes wide as the steering angle grows in either direction.

Figure 13 shows variation of ramp climbing ability for various steering angles. The inclination angles of the ramp were chosen for 5, 10, 15 and 20 degrees. For all slopes the motor torques are kept constant at the same value. As shown in Fig. 7, as the steering angle increases toward + ϕ_{max}, the force ratio in the y-axis, which is directed up the slope in this experiment, grows. It is seen in Fig. 13 that the robot can climb up a steeper slope as the steering angle increases. In the figure, the values marked as 'x' are measured value, while the solid line represents the theoretical value computed from consideration of the gravitational force. It follows that the ramp climbing ability improves with the steering angle for the identical motor torques.

7. Conclusions

In this research a four-wheeled omnidirectional mobile robot equipped with variable wheel arrangement mechanism (VWAM) has been developed. The VWAM, which can function as a continuously-variable transmission, is designed so that the wheel modules rotate about the corners of the robot body, thus providing structural stability independent of wheel arrangements. The steering range, therefore, has been significantly increased, which leads to extension of the velocity ratio from the wheel velocities to robot velocity. Due to this feature, the size of an actuator to meet the specified performance can be reduced or performance of the mobile robot such as gradability has improved for given actuators.

References

[1] Blumrich, J. F., "Omnidirectional vehicle," *United States Patent* 3,789,947, 1974.

[2] Ilou, B. E., "Wheels for a course stable self-propelling vehicle movable in any desired direction on the ground or some other base," *United States Patent* 3,876,255, 1975.

[3] West, M., Asada, H., "Design of ball wheel mechanisms for omnidirectional vehicles with full mobility and invariant kinematics," *Journal of mechanical design*, pp.119-161, 1997.

[4] Wada, M, Mory, S, "Holonomic and omnidirectional vehicle with conventional tires," *Proc. of ICRA*, pp. 3671-3676, 1996.

[5] Carlisle, B., "An omnidirectional mobile robot," *Development in robotics*, Kempston, pp. 79-87, 1983.

[6] Pin, F., and Killough, S., "A new family of omnidirectional and holonomic wheeled platforms for mobile robot," *IEEE Transactions on Robotics and Automation*, Vol. 15, No. 6, pp. 978-989, 1999.

[7] Muir, P., and Neuman, C., "Kinematic modeling of wheeled mobile robots," *Journal of Robotic Systems*, Vol. 4, No. 2, pp. 281-340, 1987.

[8] Asama, H., Sato, M, Bogoni, L., Kaetsu, H., Masumoto, A., and Endo, I., "Development of an omnidirectional mobile robot with 3 DOF decoupling drive mechanism," *Proc. of ICRA*, pp. 1925-1930, 1995.

[9] Wada, M., and Asada, H., "Design and control of a variable footprint mechanism for holonomic omnidirectional vehicles and its application to wheelchairs," *IEEE Transactions on Robotics and Automation*, Vol. 15, No. 6, pp. 978-989, 1999.

[10] Tahboub, K., and Asada, H., "Dynamic analysis and control of a holonomic vehicle with continuously variable transmission," *Proc. of ICRA*, pp. 2466-2472, 2000.

[11] Byun, K.S., Kim, S.J., and Song, J.B., "Design of continuous alternate wheels for omnidirectional mobile robots," *Proc. of ICRA*, pp. 767-772, 2001.

[12] McKerrow, P. J., *Introduction to Robotics*, Addison-Wesley, 1991.

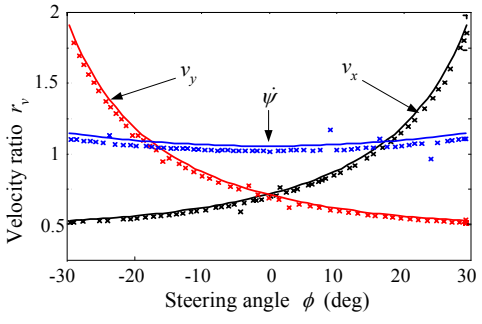

Fig. 12 Experimental results for measurement of velocity ratios.

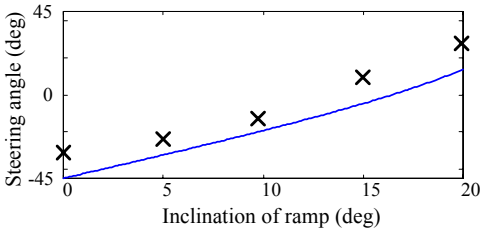

Fig. 13 Experimental results for ramp climbing ability.